Effect of the supplementation with a blend containing short and medium chain fatty acid monoglycerides in milk replacer on rumen papillae development in weaning calves

Title: EFFECT OF the supplementation with a BLEND containing short and medium chain fatty acid monoglycerides in MILK REPLACER ON RUMEN papillae DEVELOPMENT IN weaning CALVES

Author: L. Ragionieri A. Cacchioli F. Ravanetti M. Botti A. Ivanovska R. Panu F. Righi A. Quarantelli F. Gazza

PII: S0940-9602(16)30094-2
DOI: http://dx.doi.org/doi:10.1016/j.aanat.2016.04.035
Reference: AANAT 51047

To appear in:

Received date: 29-10-2015
Revised date: 17-3-2016
Accepted date: 21-4-2016

Please cite this article as: Ragionieri, L., Cacchioli, A., Ravanetti, F., Botti, M., Ivanovska, A., Panu, R., Righi, F., Quarantelli, A., Gazza, F.,EFFECT OF the supplementation with a BLEND containing short and medium chain fatty acid monoglycerides in MILK REPLACER ON RUMEN papillae DEVELOPMENT IN weaning CALVES, *Annals of Anatomy* (2016), http://dx.doi.org/10.1016/j.aanat.2016.04.035

Ragionieri L., Cacchioli A., Ravanetti F., Botti M., Ivanovska A., Panu R., Righi F., Quarantelli A., Gazza F.

Department of Veterinary Sciences, University of Parma, Via del Taglio, 10, 43126 Parma, Italy

Corresponding author: Francesca Ravanetti, Department of Veterinary Sciences, University of Parma, Via del Taglio, 10, 43126 Parma, Italy. E-mail: francesca.ravanetti@unipr.it

EFFECT OF THE SUPPLEMENTATION WITH A BLEND CONTAINING SHORT AND MEDIUM CHAIN FATTY ACID MONOGLYCERIDES IN MILK REPLACER ON RUMEN PAPILLAE DEVELOPMENT IN WEANING CALVES.

Summary

Feeding of neonates with artificial milk formulas is a popular trend towards early weaning of newborn dairy calves. These milk replacers (MR) should accelerate the rumen development, determining early solid feed intake and leading to better performances in cattle. Previous research demonstrated that sodium butyrate supplementation in MR can affect both small intestine and rumen development. Also acetate and propionate showed similar properties, while only a few studies indicate some potential benefit of monoglycerides on gut functions. The present study is aimed to determine the effect of the supplementation of a blend containing short and medium chain fatty acids monoglycerides (SMCFA) in milk replacer on rumen papillae development and growth performances in weaning calves.

Twenty bull calves (about 2 weeks old, weighing around 43 Kg) were randomly allocated into two groups: Control (C) and Treated (T). Besides MR and starter diet, the latter offered at libitum, T calves received 0.2 % SMCFA in MR. Animals were slaughtered after 56 days from the beginning of the trial.

No difference was found between groups either in growth performances or in mean number of papillae/cm^2 of mucosa, total surface of papillae (mm^2)/cm^2 of mucosa or papillary size. In both groups, the morphology of the rumen epithelium was typical of parakeratosis. The cells of the stratum spinosum were directly transformed into swollen, ovoid, still nucleated keratinocytes, particularly at the papillary tip, probably as a result of unphysiological osmolarities caused by high concentrate intake. Degenerated squamous horn cells covered the “balloon like” cells forming several layers, particularly in the places of the rumen mucosa more protected from an abrasive action of solid feed. This was more evident in C animals. The squamous cells covering the papillary tip showed cytoplasmic protrusion, representing remains of the attachment sites of desmosomes, which increased the total absorptive surface and were more numerous and higher in T compared to C animals. It might be hypothesized that SMCFA supplementation in MR could better regulate epithelial cell proliferation and probably have an “emollient effect” leading to an easier “peeling” that might increase efficiency for nutrient transport across the epithelium.

Keywords: rumen papillae, calves, short and medium chain fatty acids monoglycerides, histology, SEM, TEM

1. INTRODUCTION

The particular development of the cattle digestive system requires about ten months to be completed and the weaning phase represents the most critical period. Moreover weaning has been demonstrated to deeply affect long term performance and health status of the animal (Soberon et al., 2012). Among weaning strategies, feeding newborn calves with a limited amount of whole cow's milk (WM) or milk replacer (MR) and free-choice starter mixture is the most common practice. The aim of this strategy is to speed up rumen development and decrease the weaning age of calves, but implies a special attention to the composition and structure of the solid feed offered, that is the main stimulator of rumen development, as ruminal papillae start to grow just when the milk-fed calves begin to eat solid feed (Zitnan et al., 1999). On the other hand, when, for managerial and economic reasons, it is not possible to provide the newborns WM, particular attention must also be payed to the composition of the MR, especially when it contains plant proteins (Seegraber and Morril, 1986; Mir et al., 1991; Montagne et al., 1999; Drackley et al., 2006; Gorka et al., 2011a) commonly used as cheaper substitutes of milk proteins. Until solid feed intake starts, liquid feed, mainly digested in the abomasum and small intestine, is the sole source of nutrients for newborn calves. Small intestine development affects milk digestion and nutrient absorption influencing calf growth and health status in the first weeks of life and, therefore, also feed intake and, indirectly, rumen development. In contrast to WM, MR can contain anti-nutritional factors and lacks bioactive substances normally present in WM (e.g., hormones and growth factors) (Seegraber and Morril, 1986, Blattler et al., 2001, Gorka et al., 2009; Guilloteau et al., 2009,) providing less stimulation toward abomasum and small intestine development. This may also reduce starter mixture intake, thereby slowing rumen development (Gorka et al., 2009).

For these reasons, new formulas of artificial milk, starter mixture and new additives are currently being investigated in order to improve the calf nutritional regime and, consequentially, decrease mortality and morbidity, increase post-weaning rate of gain and significantly decrease replacement costs in dairy enterprises (Baldwin et al., 2004).

MR should have chemical-physical characteristics and nutrient content as close as possible to those of the WM, in order to maximize absorption and prevent gastrointestinal diseases, which, together with respiratory syndromes, are common in calves and usually lead to the massive use of antibiotics. This practice is, in fact, often preferred over proper prophylactic and managerial control, with the consequence of increasing the problem of antibiotic resistance, which especially affects the newborn calf. For this purpose, milk and starter diet (SD) may be enriched by probiotics

(Agazzi, 2014) and prebiotics, or by nutrients with a proven prebiotic activity such as sodium butyrate (Gorka et al., 2011a, Gorka et al., 2011b, Gorka et al., 2014). The latter, added to calves diet, has been demonstrated to positively affect rumen papillae development, also when added only to the MR. Evidence for a similar activity of acetate and propionate has been reported for both in calves (Sakata and Tamate, 1979) and in vivo on rats (Sakata, 1987). Among lipid additives some trials have been conducted using a blend of monoglycerides of short and medium chain fatty acids (SMCFA) and observing its effects on the gastrointestinal tract (Garret and Grisham, 1999; Zentek et al., 2012; Jacobi and Odle, 2012). SMCFA are fatty acid monoesters of glycerol usually found in very low amounts in cell extracts, as intermediate products in the degradation of triacylglycerides, but are also industrial products containing waste oils. As reviewed by Garret and Grisham (1999) they easily form micelles in aqueous solutions, are rapidly absorbed by intestinal epithelium, possess detergent properties and have antimicrobial activity against various bacteria (Batovska et al., 2009; Namkung et al., 2011). We hypothesize that SMCFA could represent a further additive potentially improving weaning performances of calves through action on ruminal epithelial cells. The aim of our trial was to test the effects of the addiction of SMCFA to MR on weaning calves rumen development, paying particular attention to the effect on rumen papillae histomorphology.

2. Materials and methods

The present study complied with the Italian rules on animal welfare. It was conducted as a completely randomized block design on 20 Italian Holstein male calves. The calves were selected in 2 dairy farms located in Parma Province (Italy) and were born from multiparous cows (3-4th lactation) homogeneous for productivity, body weight and genetics. The animals were enrolled in the study at an average of 2 weeks of age and divided into two homogeneous groups (Control –C- and Treated –T-). Each group included animals from both farms in equal number, and the mean body weight (BW) was 42.8 ± 1.5 Kg for C and 42.7 ± 1.7 for T group. The calves were previously fed 2 L of colostrum within four hours and other 4 L within 12 hours from the birth. At their arrival, calves were housed individually in 1.20 X 1.40 m pens grouped in the number of five (corresponding to a single replicate) in boxes with natural ventilation, natural lighting and no humidity and temperature control. Bedding consisted of wood shavings that were partially renewed daily. Before the test, calves underwent an adaptation period of n. 3 days, during which they were administered 3 L of MR at the concentration of 12% twice daily (CombiMilk® Emilatte

Premium, CAP, Parma, Italy) containing 25% crude proteins (CP) and 22% crude oils and fats (FAT). Calves were then observed for 56 days. During the trial, the same MR was administered at the total dose of 3 L (12% concentration) twice daily at 7:00 a.m. and 19:00 p.m. in a bucket provided of a calf latex rubber feeding nipple, at the temperature of 40°C. A pelleted starter feedstuff (Mix Starter vitelli CUB S.C. 25, cap, Parma, Italy) containing 18% CP and 3.4% FAT, was offered *ad libitum* starting from the first day of the trial in the stainless steel manger located in the front side of the individual pen. Fresh water was available *ad libitum* in a bucket located adjacent to the manger for the entire period. Neither roughage nor forage was offered during the entire period. Calves of the T group received 11 g/day of monoglycerides containing short and medium chain fatty acids emulsified in the milk replacer during the whole trial. Calves of the C group received additional 18 g of milk replacer powder to obtain an isoenergetic liquid diet. At the end of the trial, the animals were sent to the slaughterhouse for post-mortem sampling and evaluations.

2.1 Performances and development measurements

Shrunk BW (weight before morning feeding) was measured at the arrival for group allotment, at the start of the trial and weekly during the entire trial, using a calibrated electronic scale. Hip width (HP), hearth girt (HG) circumference and wither height (WH) were measured at the same intervals as primary indicators of skeletal growth.

Body weight gain (BWG) was expressed at 56 days of trial. The average daily live weight gain (ADG) was then calculated dividing BWG by the trial length (56 days). Starter diet intake (or feed intake (FI)) was measured weekly by difference between administration and residues to evaluate the feed conversion efficiency (FCE) calculated as BWG/FI. Performances and development measurements were performed on all animals independently of the occurrence of diseases not related to the gut (e.g. respiratory diseases).

2.2 Tissue sampling and analysis

At the end of the trial all calves were sent to the slaughterhouse before the morning feeding, killed by captive bolt stunning and exsanguinated. The rumen, reticulum, omasum, abomasum, small intestine and large intestine were collected, separated, emptied, rinsed repeatedly with water to remove the ingesta, drained, and individually weighed. In particular, the rumen of each animal, was removed and opened by a horizontal incision along the left side of the ventral sac. After the removal of the ingesta, composed of fermented feedstuff, hairs in small amount and fluid milk residues, three whole thickness samples of one square centimeter from corresponding sites of the

left side of the cranial dorsal sac of the rumen were collected, similarly to Gorka et 2009 and Gorka et al., 2011b. The first sample was processed for routine preparation of paraffin embedded tissues for histology; the second was processed for scanning electron microscopy (SEM), the third for transmission electron microscopy (TEM).

2.3 Histological evaluation and Histomorphometry

A sample from each animal was immersed in 4% buffered formaldehyde for 5 d, after being fixed with pins on cork discs to prevent shrinkage. Then the samples were rinsed with water and photographed at 0.8x magnification using a light stereomicroscope (Nikon SMZ 1000, Tokyo, Japan) equipped with a digital camera (Nikon model DS-5M) and an image analysis software (NIS – Elements AR 3.1, Nikon Tokyo, Japan), to evaluate the density of papillae (number of papillae / cm^2 mucosa) (PD), their gross morphology, color and clumping. Macroscopic observations with attention paid to grooves covering papillary surface were also done.

Subsequently, the samples were dehydrated in ethanol and embedded in paraffin. Histological sections (9 µm thick) were then stained with hematoxylin and eosin (H&E) for morphometric analysis under a light microscope Nikon Eclipse 90i (Nikon, Tokyo, Japan) equipped with the same digital camera and image analysis software of the stereomicroscope.

Five papillae (selected randomly) were measured for each animal (50 papillae per group of treatment). The following morphometric parameters were measured: papillae length (PL) (distance between the base and the tip of the papillae) and width (PW) (at the middle of the papillae), total surface of papillae per cm^2 mucosa (TS) (determined as length x width x 2, multiplied by PD) and epithelial layer thickness. In each papilla, 3 regions of mucosa (papillary tip (T), papillary base (B) and interpapillary mucosa(I)), as indicated in fig. 1A, were observed.

On each location, the following parameters were measured at 40x magnification (fig. 1B): thickness of the *stratum basale* (SB) + *spinosum* (SS) + *granulosum* (SG), thickness of the *stratum corneum* (SC), number of layers of different types of cells of the SS, SG and SC (for this layer, vacuolated, balloon cell-like, horn cells (SC bal) and flattened cornified, squamous, cells (SC sq) were counted separately (see fig. 1B)).

Only at the tip of the papillae, the length of the papillary bodies and the extensions (maximum and minimum) of the epithelium into the *lamina propria* (epithelial pegs) (fig. 1C) were also measured.

Moreover a classification of the different papillary shape and size, including the presence of waved sides (secondary papillae) and of interposed papillae observed in the interpapillary regions was made to perform comparison between the two experimental groups.

2.4 Scanning Electron Microscopy (SEM) analysis

The second sample collected from each animal was processed for a SEM view of both grooves and micro-papillae covering papillary surface. They were immediately immersed in a fixative (2.5% glutaraldehyde in 0.1 M sodium cacodylate buffer, pH 7.2) at 4°C. Once fixed, the samples were washed in 0.1 M sodium cacodylate buffer and dehydrated in increasing concentrations of ethanol. The samples were then critical-point dried in carbon dioxide, attached to stubs and coated with gold-palladium in a sputtering device (SCD 040 Balzer Union, Liechtenstein). Specimens were examined and photographed with a scanning electron microscope Zeiss DSM 950 (Zeiss, Germany) operating at 10 keV.

2.5 Transmission Electron Microscopy (TEM) analysis

The third sample was fixed in 2.5% glutaraldehyde in 0.1M sodium cacodylate buffer (pH 7.2) for 24 hours, then postfixed with 1% osmium tetroxide, subsequently dehydrated with acetone and embedded in Durcupan (Fluka Chemie, Buchs, Switzerland). Ultrathin sections (~ 70 nm) were cut with a diamond blade, stained with 3% uranyl acetate and lead citrate and observed by a JEOL transmission electron microscope (JEM 2200 FS, Tokyo, Japan) operating at 80KeV.

2.6 Statistical analysis

The statistical assessment was founded on the mean values per animal. The results are shown as mean average ± standard error (SE). Values were analyzed by analysis of variance procedure (ANOVA). When ANOVA was significant, Tukey's post-hoc tests were carried out in order to study the significant differences among the distinct groups.

Regression analysis was used to determine relationships between two different parameters across all calves and experiments. Linear models were initially fit, subsequently followed by higher order models if applicable. The test of Parallel Lines was used to compare the slope coefficients between the two experimental groups.

All analyses were performed with PAST statistical software package version 3.0 (http://folk.uio.no/ohammer/past) (Hammer, 2001). Statistical significance was assigned to $p<0.05$.

3. RESULTS

3.1 Performances and development

The mean values of the measured indicators of skeletal growth, BW, ADG and FCE in C and T calves are shown in *Table 1*. The mean BWG of the T animals reached 34.34 ±3.2 Kg during the trial period, while for C group it was slightly larger 39.03±4.3. However, the difference between the BWG of the two groups was not statistically significant and also the final BW of T and C animals did not result in a significant difference. Similarly, no significant effect of the supplementation of the MR with SMCFA was found comparing all the parameters (*see table 1*). During the trial, two T calves showed chronic respiratory disease which induced a depressed growth.

TABLE 1. Morphometric and zootechnical parameters of the calves (Mean ± S.E.)

PARAMETER	CONTROLS	TREATED	ANOVA (P)
body weight (BW) (Kg)	82.4 ± 5.4	77.8 ± 4.5	N.S.
heart girth (cm)	98.7 ± 2.2	97.2 ± 1.8	N.S.
withers height (cm)	90.9 ± 1.2	90.9 ± 1.3	N.S.
hip height (cm)	93.8 ± 1.3	93.7 ± 1.3	N.S.
rump width (cm)	22.5 ± 0.5	22.1 ± 0.5	N.S.
Feed Conversion Efficiency (FCE)	1.3 ± 0.1	1.7 ± 0.3	N.S.
Average Daily live weight Gain (ADG)	0.7 ± 0.1	0.6 ± 0.1	N.S.

3.2 Rumen development

The mean empty rumen weight (RW) of SMCFA supplemented animals was slightly greater (1080.7 ±150.8) compared to that of C calves (963.7 ±112.8). However the difference was not significant. No significant differences between the two groups were found (*Table 2*) either when RW was expressed as percent of BW or as percent of whole intestine weight. Moreover, when RW and the weight of the intestine were correlated, they resulted in a directly proportional increase in both groups. However, although regression analysis explained this better in T ($p<0.01$) than in the C group ($p<0.05$), the test of Parallel Lines, used to compare the slope coefficients between the two groups, did not show significant differences.

3.3 Macroscopic and microscopic characteristics of ruminal papillae

The density and gross morphology of the papillae stereo-microscopically observed on the samples obtained from identical sites of the rumen dorsal sac was quite variable within both experimental groups. (figs. 2 and 3). PD varied from 48 to 202 papillae per cm^2 of mucosa, PL from 0.85 to 2.8 mm, PW from 1.46 to 4.98 mm and TS from 11.6 to 318.3 mm^2 / cm^2 of mucosa. No statistically significant (N.S.) difference was found comparing PD, PL, PW and TS between T and C animals (*Table 2*).

TABLE 2. Morphometric parameters of the rumen and rumen mucosa (Mean ± S.E.)

PARAMETER	CONTROLS	TREATED	ANOVA (P)
Rumen Weight (g) (RW)	963.7 ±112.8	1080.7 ±150.8	N.S.
% Rumen / whole intestine weight	16.5% ± 1.3%	15.8% ± 1.2%	N.S.
% Rumen / body weight	1.3% ± 0.1%	1.2% ± 0.1%	N.S.
Papillae Density (number/cm^2) (PD)	108.3 ± 12.9	115.9 ± 13.4	N.S.
Papillae Length (mm) (PL)	1.98 ± 0.2	2.01 ± 0.2	N.S.
Papillae Width (mm) (PW)	0.3 ± 0.02	0.3 ± 0.02	N.S.
Total Surface (mm^2/cm^2 mucosa) (TS)	121.9 ± 13.6	145.7 ± 17.8	N.S.

Moreover, PL and PD were found to be inversely proportional. Although the strength of the linear relationship between the two variables was greater for T ($p<0.01$) than for C calves ($p<0.05$), the test of parallel lines did not highlight significant differences between the slope coefficients of the two groups. Similarly a negative correlation without significant differences between T and C animals, was found testing the relationship between PD and BW, RW or ADG (fig. 4). On the contrary, a direct relationship was found between PL and BW, RW, and ADG (fig. 5). Also, in these cases, the p values were smaller for T animals, but no significant differences between the slope coefficient of the two groups were found with the test of Parallel Lines.

In both groups, in stereomicroscopic and SEM (fig. 6) images, the papillae showed an approximately flattened tongue-like appearance and had their greatest thickness at about two-thirds of their length. The papillae were generally characterized by the presence of ridges and

grooves on their entire surface. When they were observed with light microscopy (fig. 7), their surface was irregular-shaped with very irregular or waved sides and short interpapillary distances. A few papillae branched into small secondary papillae at the base of the primary ones. Moreover, interposed papillae were also observed in interpapillary regions.

3.4 Rumen mucosa

Rumen mucosa of weaning calves was outlined by a stratified, cornified squamous epithelium and a *lamina propria* of connective tissue. In standard histological preparations only parts of the calves papillary epithelium showed the four classical distinct cell layers, three of which composed of nucleated "living" cells (from the *lamina propria* towards the luminal surface: SB, SS and SG superficially covered by a more or less thin layer of dead or degenerating cells (SC). In many areas, instead, over a layer of dark columnar cells of the SB, only numerous rows of large pale polygonal cells with eccentrically placed nuclei were visible. This "intermediate layer" was bounded, on the luminal side, by a relatively inconspicuous zone of flattened cells which might correspond to the SC of the adult (Fig. 8).

The SB contained a single layer of cubic or cylindrical cells with their longitudinal axis at right angles to the basement membrane. The SS, was composed, deeply, of oval cells that, moving superficially, became horizontally flattened, presenting large rounded nuclei. The SG, when distinguishable, contained thickened cells, arranged parallel to the luminal surface and with nuclei which began to degenerate. The SC was characterized by both plate-shaped corneal cells (SC sq) and voluminous "balloon-shaped" cells (SC bal). With light microscopy it was quite difficult to identify, among SC sq, type A or type B cells, according to the description given by Zitnan et al. (1999). Conversely voluminous "balloon-shaped" corneal cells of type C (parakeratotic), with wide spaces around their nuclei and poorly stained cell material only in their periphery, were arranged on one or more layers between the SS (or the SG, when present) and the SC sq.

The thickness of SC (dead or degenerating cells) and that of the layers of living nucleated cells (SB+SS+SG) was measured in 3 different regions of mucosa (Fig. 1 A, B and Fig. 9). Although the mean values of thickness of SC and those of SB+SS+SG, in the different measurement points, were generally larger for T than for C animals, a significant difference resulted only comparing the data of the living cells of the two groups in the interpapillary mucosa ($p<0.05$ ANOVA and Tukey's post-hoc test).

At the papillary tip, epithelial pegs and papillary bodies were well developed and generally their mean measures were larger in C than in T animals (Fig. 10). However, comparing their extensions, only the length of papillary bodies were significantly larger in C animals (ANOVA and Tukey's post-hoc test, $p<0.05$).

As the cells of the different layers may have different sizes, to evaluate whether the differences in the epithelium thickness could be due to the cell size or to the number of cell layers within each stratum, the latter was measured in the same 3 different positions (papillary tip, papillary base and interpapillary mucosa) (Fig. 11), obviously omitting the counts in the SB which is always constituted by a single row of cells. The results and the significant differences found with ANOVA and Tukey's post-hoc test are shown in Figure 12. In both C and T calves the number of layers of SC bal is significantly greater at the papillary tip and smaller at the papillary base and in the interpapillary spaces. Instead, the number of SC sq cells layers gradually increases moving from the tip to the base of the papillae and then in the interpapillary mucosa, but without significant differences within both T and C group. While comparing C and T animals, either at the papillary base or in the interpapillary region, C animals show a significantly greater number of layers of SC sq cells.

Desquamation of the superficial horn cells was also clearly visible when the papillary tips were observed with SEM (Fig. 13). Moreover, at high magnification, SC sq cells have a distinctly granular appearance due to the presence of nipple-like projection or cytoplasmic protrusions (microvilli-processes) covering cell surfaces. When their mean density was evaluated on 100 μm^2 areas, the results were significantly greater (ANOVA $p<0.001$) in T (619.2±9.3) compared to C animals (487.5±9.3).

3.5 TEM analysis

TEM analysis was conducted on the epithelial cells from the papillary tip, in T and C animals.

The four cell layers (SB, SS, SG and SC) which, under the light microscope, seemed to merge into one another without distinct boundaries, also showed similar features when observed with TEM. At ultrastructural analysis, in fact, only the boundary between the two intermediate layers is indistinct, while the limits of the SB and SC are relatively clearly defined.

SB cells (Fig. 14) were cuboidal or columnar with their long axes disposed at right angle to the basement membrane and many mitochondria arranged below their ovoid nuclei. Cytoplasmic processes extended from the cell base towards the basement membrane and into the lateral

intercellular spaces. Some cells showed a relatively pale nucleus (containing both euchromatin and heterochromatin), while their cytoplasm was darkly stained and contained clear vesicles and small mithocondria, other cells had darkly stained nucleus, but pale cytoplasm (Fig. 14 A, B, C and Fig. 15 A).

SS cells (Fig. 15 B) had oval nuclei with evident nucleoli, very few mitocondria, accumulation of fine granular material and serrated outline, due to radially arranged cytoplasmic processes, which are attached, by obliquely placed desmosomes, to similar processes from neighboring cells (Fig. 15 D). Further accumulation of granular material continued as the cells became flattened horizontally in their passage towards the lumen.

SG cells lay parallel to the luminal surface, separated by small intercellular spaces. They showed degenerating nuclei and many more fibrils in the peripheral cytoplasm (Fig. 15 B, C). The granule-containing endoplasmic reticulum seemed to swell, often displacing the nucleus towards one end of the cell. Towards the outer limit of this layer (which is directly below the SC) the intercellular spaces were largely obliterated by the fusion of adjacent cell membranes (Fig 15 E, F).

The transition to the SC was abrupt (Fig. 16 A, E). The tight junctions between the cells opened out, and the intercellular space was once more present (Fig. 16 B, F, G). Very few nuclei persisted in this layer, and the majority of cells showed a central core of fine granular material surrounded by peripheral fibrils. Some cells showed a predominance of centrally placed fine granules and striped-spongious cell material in their periphery. They were distinguishable as Type C ("ballooned" or "parakeratotic" cells), while other cells in which the cisternae of the endoplasmic reticulum had not reached maximum development were flattened (Fig. 16 E). Between the flattened cells, desmosomes, as such, disappeared, and the cells were often held together by interdigitating processes (Fig. 16 C, D) that, besides increasing the cell surface by many times in size, ultimately interlock the outer part of the epithelium into a cohesive and protective stratum corneum. When desmosomes break down to allow the surface layer of SC to slough off, they leave the former attachment sites as processes scattered over the surface of the cells (Fig. 16 B, F, G, H). As previously seen for SEM images, these protrusions in C seem to be less dense than in T animals. Large number of microorganisms was found over the surface of the epithelium. The most luminal horn cells exhibited large cavities (lysosome-like structures or membrane-bound granules) and denser peripheral cytoplasm containing fine both fibrillary and granular material (Fig. 16 G, H). Amorphous material was visible in the intercellular spaces between SC cells. It might come from the degraded organelles of the granular cells, which undergo transformation process to horn cells.

4. DISCUSSION

To our knowledge, this study is the first one to analyze the effects of the addiction of SMCFA to MR on weaning calves growth performances, focusing on papillae rumen development.

Previous studies have shown that calves diet supplementation with additives like sodium butyrate in MR has a positive indirect effect on rumen development (Gorka et al., 2011b, Gorka et al., 2014), probably because of their positive effect on performance and health of calves.

Results of the present study did not highlight significant positive effects of SMCFA supplementation to the MR at the dose tested on the growth performances of calves; however it should be considered that two animals of the T group had chronic respiratory disease that decreased their growth performances. This explains the numerically lower mean values of skeletal growth parameters, mean BWG and ratio between RW and whole intestine weight or body weight of T compared to C calves. These animals were included in the study independently from their effect on the group performances because they never interrupted milk consumption, ensuring the activity of the tested product on their gastrointestinal tract. Thus we assumed that the histomorphological evaluations, which were the main goal of the present trial, were not affected by the respiratory disease. Instead, solid feed FCE and absolute RW as well as the values of the parameters related to ruminal papillae resulted slightly higher in T calves. It is conceivable that, since abomasum and small intestine are the primary responsible for milk digestion, SMCFA supplementation, as expected, exerted a direct effect primarily on the lower gastro-intestinal tract. Abomasum and intestine, in fact, were in proportion slightly heavier than rumen in T compared to C group. Moreover, it is possible that SMCFA supplementation in MR was also beginning to produce an indirect positive effect on the rumen of T animals, favoring their capabilities of absorbing energy sources also from solid feed. In addition, a direct effect of the additive on the same organ cannot be excluded since milk residues were found in the rumen at slaughter. This could explain the slightly greater values of all the parameters related to rumen, its internal surface and FCE.

In both T and C calves, ADG resulted positively correlated to PL and negatively correlated to PD. Therefore, assuming a similar energy uptake between groups from milk, animals with longer and less numerous papillae and, in general, a larger absorbent surface per unit area of the rumen showed numerically higher growth performances. The morphology of the papillae with waved surfaces, the presence of small interposed papillae, as well as the presence of cytoplasmic

protrusion on the horn cells at the papillary tip, might indicate a need of amplifying the absorbent surface of the ruminal mucosa. This is probably due to the great availability (*ad libitum*) of SD, that is a concentrate, or finely ground, highly digestible ration and may have stimulated ruminal mucosal proliferation as an adaptive response to enhance metabolism. The large amount of soluble substrate available for fermentation in the rumen likely resulted in hyperplasia of metabolically active cells (Bull et al., 1965; Dirksen and Garry, 1987; Siddig Ahmed, 2007) with the consequence that, during the cornification process, the SG disappeared or was reduced to small numbers of cells, and SS cells were directly transformed in swollen, ovoid, still nucleated keratinocytes of a thickening SC. According to Marcato (2000), this morphology is typical of parakeratosis and could be predisposed by vacuolization of epithelial cells as a result of unphysiological osmolarities caused by high concentrate intake (Hinders and Owen, 1965; Nocek et al., 1984). Effectively, SC bal formed more layers at the papillary tips, that are the main parts of the rumen in contact with the fermenting ruminal contents. On the other hand, SC sq were arranged on a gradually greater number of layers moving towards the papillary base and the interpapillary mucosa, that are places more protected from the impact with solid feed and, therefore, from the abrasive action of the digesta on the exposed horn cells surface. In any case, it is well known that concentrated fed animal lack of effective fiber and this results in an excessive thickness of the epithelium (Scott and Gardner, 1973) that lowers both the efficiency for nutrient transport across it and the metabolic activity per unit weight (Nocek et al., 1980). In addition, epithelial hyperkeratinization may be one of the reasons for the non-uniformity in length, abnormal and randomized growth and clumping of papillae, that could lead to their atrophy (Gaebel et al., 1987; Nocek and Kesler, 1980; Sherwood et al., 2006). Although the papillae morphology is quite variable and not significantly different in T and C animals, because of the higher proportion of keratinized cell layers, the latter seem to be more likely destined to suffer, in time, the negative effects of parakeratosis, while T animals are expected, over times longer than that of the experimentation, to improve their FCE. These results are consistent with reports from Sakata and Tamate, (1978; 1979), which indicated how a possible effect of SMCFA supplementation seems to be a better regulation of cell proliferation and, according to Garret and Grisham (1999), it is even conceivable an “emollient effect” leading to an easier “peeling” of the SC. This could also explain the observation of the cytoplasmic protrusions on the horn cells of T animals, that are more numerous and apparently higher compared to those of C group. As they should represent remains of the attachment sites of desmosome, an increased sloughing of

necrotic cells preserve the former attachment sites as bigger processes scattered over the surface of the cells (Scott and Gardner, 1973) which, in turn, increase the absorption surface improving the transport function of the epithelium.

Finally, the greater length of the papillary bodies at the papillary tip observed in C, might be related to the need of decreasing distance between basal epithelial cells and capillaries to increase ion exchange and the transport capacity of nutrients at least in the parts of the mucosa in which there is a relative reduction of the physical barrier either to acid transport or to incoming transportable and/or metabolizable substrates (Galfi et al., 1988). This intense activity of the basal cells of rumen epithelium in storage and transport of metabolites between the lumen of the rumen and the circulatory system could be also proved by the abundant presence of metabolic organelles and of large vesicles, more easily visible in the dark basal cells. These organelles are typical of the basal cells of the rumen mucosa, differently from those of other keratinizing and mucus-forming epithelia, and are indicative of its absorptive properties (Lavker et al., 1969).

5. CONCLUSIONS

Calves receiving SMCFA added to MR at the dose of 11g/day for a period of 56 days from their second week of life, did not show any difference in growth performances when compared with the control animals. From a histological point of view, T calves showed a lower amount of degenerative tissue accumulation and a higher number of cytoplasmic protrusions on the exposed horn surfaces. This could lead to a higher efficiency of absorption with a higher FCE and a potentially improved post-weaning development. The rumen development and the histological effects of SMCFA addition to MR have, however, to be further studied both at different doses and on different intervals during the weaning period; moreover the evaluation of additional parameters, such as mitotic and apoptotic indexes, should be considered.

Acknowledgements

The authors gratefully thank Alessandro Zappino, Irene Enfiomusi and Massimiliano Festuccia, for the work done during the trial and Giuliano Alba and Andrea Rossi for the technical assistance. Financial support by SILO S.p.A. (Firenze) is gratefully acknowledged. The funders had no role in the study design, data collection and analysis, decision to publish, or preparation of the manuscript.

REFERENCES

Agazzi A., Tirloni E. Stella S., Maroccolo S., Ripamonti B. Bersani C., Caputo J.M., Dell'Orto V. Rota N., Savoini G., 2014. Effects of species-specific probiotic addition to milk replacer on calf health and performance during the first month of life. Ann. Anim. Sci., 14, 1, 101-115.

Baldwin R.L.VI, McLeod K.R., Klotz J.L., Heitmann R.N., 2004. Rumen Development, Intestinal Growth and Hepatic Metabolism In The Pre- and Postweaning Ruminant. J. Dairy Sci., 87, E55-E65.

Batovska D.I., Todorova I.T., Tsvetkova I.V., Najdenski H.M., 2009. Antibacterial study of the medium chain fatty acids and their 1-monoglycerides: individual effects and synergistic relationships. Pol J Microbiol., 58,1, 43-47.

Blättler U., Hammon H.M., Morel C., Philipona C., Rauprich A., Romé V., Le Huërou-Luron I., Guilloteau P., Blum J.W., 2001. Feeding colostrum, its composition and feeding duration variably modify proliferation and morphology of the intestine and digestive enzyme activities of neonatal calves. J. Nutr., 131, 1256-1263.

Bull L.S., Bush L.J., Friend J.D., Harris B., Jones E.W., 1965. Incidence of ruminal parakeratosis in calves fed different rations and its relation to volatile fatty acid absorption. J Dairy Sci, 48, 1459-66.

Dirksen G., Garry F.B., 1987. Diseases of the forestomachs in calves. Continuing Education, 9, 173-179.

Drackley J., Blome R., Bartlett K., Bailey K., 2006. Supplementation of 1% L-glutamine to milk replacer does not overcome the growth depression in calves caused by soy protein concentrate. J. Dairy Sci., 89, 1688-1693.

Gaebel G., Martens H., Suendermann M., Galfi P., 1987. The effect of diet, intraruminal pH and osmolarity on sodium, chloride and magnesium absorption from the temporarily isolated and washed reticulo-rumen of sheep. Q J Exp Physiol, 72, 501-11.

Galfi P., Neogrady Z., Kutas F., 1988. Study of the physiological factors responsible for the adaptation of ruminal mucosa in cell-culture - Preliminary report. Magy. Allatorvosok Lapja, 43, 309-311.

Garret R.H., Grisham Ch.M., 1998. Lipids. Saunder In: Biochemistry. 2nd. Edition College Publishing. Virginia. Pp. 238-258.

Gorka P., Kowalski Z.M., Pietrzak P., Kotunia A., Kiljanczyk R., Flaga J., Holst J.J., Guilloteau P., Zabielski R., 2009. Effect of sodium butyrate supplementation in milk replacer and starter diet on rumen development in calves. J. Physiol. Pharmacol., 60, 47-53.

Gorka P., Kowalski Z., Pietrzak P., Kotunia A., Jagusiak W., Zabielski R., 2011a. Is rumen development in newborn calves affected by different liquid feeds and small intestine development? J. Dairy Sci., 94, 3002-3013.

Górka P., Kowalski Z.M., Pietrzak P., Kotunia A., Jagusiak W., Holst J.J., Guilloteau P., Zabielski R., 2011b. Effect of method of delivery of sodium butyrate on rumen development in newborn calves. J. Dairy Sci., 94, 5578-5588.

Gorka P., Pietrzak R., Kotunia A., Zabielski R., Kowalski Z., 2014. Effect of method of delivery of sodium butyrate on maturation of the small intestine in newborn calves. J. Dairy Sci., 97, 1026-1035.

Guilloteau P., Zabielski R., David J.C., Blum J.W., Morisset J.A., Biernat M., Wolinski J., Laubitz D., Hamon Y., 2009. Sodium-butyrate as a growth promoter in milk replacer formula for young calves. J. Dairy Sci., 92, 1038-1049.

Hammer Ø, 2001. Past: Paleontological Statistic Software Package for Education and Data Analysis. (ed Harper DAT), pp. 1-9. Paleontologia Elettronica.

Hinders R.G., Owen F.G., 1965. Relation of ruminal parakeratosis development to volatile fatty acid absorption. J. Dairy Sci., 48, 1069-73.

Jacobi S.K., Odle J., 2012. Nutritional factors influencing intestinal health of the neonate. Adv. Nutr.,3, 5, 687-96.

Lavker R.M., Chalupa W., Dickey J.F., 1969. An electron microscopic invetsigation of rumen mucosa. J. Ultrastructure Research, 28: 1-15.

Marcato P., 2000. Anatomia e Istologia Patologica Generale Veterinaria, Esculapio, Bologna.

Mir P., Burton J., Buchanansmith J., 1991. Nutritional performance of calves fed milk replacers containing processed soybean products. Can. J. Anim. Sci., 71, 97-106.

Montagne L., Toullec R., Savidge T., Lalles J., 1999. Morphology and enzyme activities of the small intestine are modulated by dietary protein source in the preruminant calf. Reprod. Nutr. Dev., 39, 455-466.

Namkung H., Yu H., Gong J., Leeson S., 2011. Antimicrobial activity of butyrate glycerides toward Salmonella Typhimurium and Clostridium perfringens. Poult. Sci., 90, 10, 2217-22

Nocek J.E., Herbein J.H., Polan C.E., 1980. Influence of ration physical form, ruminal degradable nitrogen and age on rumen epithelial propionate and acetate transport and some enzymatic activities. J. Nutr., 110, 2355-64.

Nocek J.E., Heald C.W., Polan C.E., 1984. Influence of ration physical form and nitrogen availability on ruminal morphology of growing bull calves. J. Dairy Sci., 67, 334-43.

Nocek J.E., Kesler E.M., 1980. Growth and rumen characteristics of Holstein steers fed pelleted or conventional diets. J. Dairy Sci., 63, 249–254.

Sakata T., Tamate H., 1978. Rumen epithelial cell proliferation accelerated by rapid increase in intraruminal butyrate. J Dairy Sci., 61, 1109-13.

Sakata T., Tamate H., 1979. Rumen epithelium cell proliferation accelerated by propionate and acetate. J. Dairy Sci., 62, 49-52.

Sakata T., 1987. Stimulatory effect of short-chain fatty acids on epithelial cell proliferation in the rat intestine: a possible explanation for trophic effects of fermentable fibre, gut microbes and luminal trophic factors. Br. J. Nutr.,58,1,95-103.

Scott A., Gardner I.C., 1973. Papillar form in the forestomach of the sheep. J. Anat., 116, 255-67.

Seegraber F., Morril J., 1986. Effect of protein-source in calf milk-replacers on morphology and absorptive ability of small-intestine. J. Dairy Sci., 69, 460-469.

Sherwood L., Klandorf H., Yancey P., 2006. Fisiologia degli Animali - dai geni agli organismi. Zanichelli, Bologna.

Siddig Ahmed R., 2007. Diet-dependent morphological changes of the rumen epithelium in sheep. FU Dissertationen Online / Mycore 2.0.2 Free University of Berlin, pp. 178. http://www.diss.fu-berlin.de/2007/696/.

Soberon F., Raffrenato E., Everett R.W., Van Amburgh M.E., 2012. Preweaning milk replacer intake and effects on long-term productivity of dairy calves. J. Dairy Sci. 95, 2, 783-93.

Zentek J., Buchheit-Renko S., Männer K., Pieper R., Vahjen W., 2012. Intestinal concentrations of free and encapsulated dietary medium-chain fatty acids and effects on gastric microbial ecology and bacterial metabolic products in the digestive tract of piglets. Arch. Anim. Nutr., 66, 1, 14-26.

Zitnan R., Voigt J., Wegner J., Breves G., Schröder B., Winckler C., Levkut M., Kokardová M., Schönhusen U., Kuhla S., Hagemeister H., Sommer A., 1999. Morphological and functional development of the rumen in the calf: Influence of the time of weaning 1. Morphological development of rumen mucosa. Arch. Tierernahr., 52, 351-362.

FIGURE CAPTIONS

Figure 1. A) Sampling sites from different locations of the ruminal papilla included tip of papilla (T), base of the papilla (B) and interpapillary region (I). B) Measurements of the epithelium included thickness of the *stratum corneum* (SC) (dead and degenerating cells), thickness of the *stratum granulosum* (SG) and *germinativum* (*stratum basale* (SB) + *spinosum* (SS)) (living cells), number of layers of cells in the SS, SG and SC. In the SC, vacuolated horn cells (balloon-like cells (SC bal) were distinguished from flattened cornified cells (SC sq). C) Total thickness of the epithelium at two levels (min and max) and length of papillary body.

Figure 2. Stereomicroscopic images of the samples of ruminal wall collected from identical sites of the left side of the cranial dorsal sac. Each rectangle refers to a control animal and shows the luminal surface (on the left) and the transversal section of the rumen wall (on the right).

Figure 3. Stereomicroscopic images of the samples of ruminal wall collected from identical sites of the left side of the cranial dorsal sac. Each rectangle refers to a treated animal and shows the luminal surface (on the left) and the transversal section of the rumen wall (on the right).

Figure 4. Negative correlation between papillae density (PD) and average daily live weight gain (ADG) in both control and treated animals. The relationship between the two variables is stronger for treated animals ($p<0.01$) than for controls ($p<0.05$). However the test of Parallel Lines did not showed significant differences between the slope coefficients of the groups.

Figure 5. Positive correlation between papillae length (PL) and average daily live weight gain (ADG) in both control and treated animals. The relationship between the two variables is stronger for treated animals ($p<0.001$) than for controls ($p<0.05$). However the test of Parallel Lines did not showed significant differences between the slope coefficients of the groups.

Figure 6. S.E.M. micrograph showing the ruminal papillae in control (A) and treated (B) animals. Papillae show an approximately flattened tongue-like appearance and are generally characterized by the presence of ridges and groves on their entire surface.

Figure 7. Micrograph showing the ruminal papillae (H&E) in control (A) and treated (B) animals. Papillae show irregular shaped or waved sides, a few branched in small secondary papillae (arrow head). Moreover interposed papillae are present in interpapillary regions (arrow).

Figure 8. Micrograph showing the epithelium of the ruminal papillae (H&E) in an adult bovine (A) and in a weaning calf (B, C). In the adult (A), the four classical layers (*stratum basale* (SB), *stratum spinosum* (SS), *stratum granulosum* (SG) and *stratum corneum* (SC) are well distinct and, in the SC, even three different types of cells, corresponding to type A, B and C classically described with TEM (Zitnan et al., 1999) are distinguishable. In weaning calves, only in certain parts (C) of the rumen epithelium were all these layers and types of cells well distinct. In many areas, instead, over a layer of dark columnar cells of the SB, there were only numerous rows of large pale polygonal cells with eccentrically placed nuclei forming the intermediate layer (IL). On the luminal side, this IL was bounded by a relatively inconspicuous zone of flattened cells corresponding to the SC of the adult.

Figure 9. Histogram showing the comparison, between control and treated animals, of the thickness of the layers of living cells (*stratum basale* (SB) + *spinosum* (SS) + granulosum(SG)) and of corneal cells (SC) in three different regions of mucosa (papillary tip, papillary base and interpapillary mucosa; see figure 1 A, B). Values are expressed as means ± SE. * = $p<0.05$ (ANOVA and Tukey's post-hoc test).

Figure 10. Histogram showing the comparisons between control and treated animals of the extensions (maximum and minimum) of the epithelium into the *lamina propria* (epithelial pegs), and the length of the papillary bodies at the tip of the papillae (see figure 1 C). Values are expressed as means ± SE. * = $p<0.05$ (ANOVA and Tukey's post-hoc test).

Figure 11. Microphotographs showing the different cell layers of the ruminal epithelium (H&E) (*stratum basale* (SB), *stratum spinosum* (SS), *stratum granulosum* (SG) and *stratum corneum (SC))* in 3 different regions of mucosa (papillary tip, papillary base and interpapillary mucosa) of controls (upper row) and treated (lower row) animals. The layers of balloon-like (SC bal) and squamous (SC sq) cells of the *stratum corneum* are clearly distinguishable.

Figure 12. Histogram showing the number of cell layers in the *stratum spinosum* (SS) + *stratum granulosum* (SG), moreover the layers of balloon-like (SC bal) and squamous (SCsq) cells of the *stratum corneum*, evaluated in 3 different regions of mucosa (papillary tip (T), papillary base (B) and interpapillary mucosa (I)) (as showed in figure 1 A). Values are expressed as means ± SE. Comparisons with ANOVA and Tukey's post-hoc test were made both among the different regions, and between controls (grey bars) and treated animals (black bars). * = $p<0.05$, ** = $p<0.01$

Figure 13. SEM micrograph showing different magnification of the squamous cells covering the tip of a ruminal papilla in control and treated animals. Rectangles indicate the area that has been magnified in the lower micrograph. Desquamation of the horn cells covering the papilla is clearly visible in the micrographs related to the treated calf. The granular appearance of the cell surface is due to cytoplasmic protrusion, representing remains of the attachment sites of desmosomes, increasing the total absorptive surface.

Figure 14. TEM micrographs of the *stratum basale* (SB) of the ruminal epithelium and of the underlying *lamina propria* (LP) at the level of the papillary tip in a treated calf observed at increasing magnifications. Rectangles indicate the area that has been magnified in the next micrograph. In the SB, dark cells with relatively pale nucleus, and paler cells with darkly stained nucleus are visible. In the dark basal cells, numerous mitocondria and clear vesicles are visible below the nucleus (A, B). Numerous cytoplasmic processes extend from the base of the cells toward the underlying connective tissue(C, D) and, within them, few small bundles of fibrils are arranged parallel to the cell membrane.

Fig. 15 TEM micrograph of cells of the *stratum basale* (A), *spinosum* (A, B), and *granulosum* (C) of the ruminal epithelium and details of intercellular junctions. Rectangles in micrograph B indicate the areas that have been magnified in the lower micrographs C and D. In D, obliquely placed desmosomes hold together two cells of the *stratum spinosum*. In E and F desmosomes and tight junctions hold together the cells of the *stratum granulosum*.

Fig. 16 TEM micrograph of cells of the *stratum corneum* of the ruminal epithelium (panoramic views A, E, G) and details of the deep interdigitations between the cells (C, D) and of the cytoplasmic processes on the horn cells surfaces (B, F, H). Their general form and ultrastructure suggested that they represent the remains of the attachment sites of desmosomes. When they break down to allow the surface layer of SC to slough off, they leave the former attachment sites as processes scattered over the surface of the cells. Note rumen microflora over the luminal surface (black arrow) and secondary lysosomes containing deposit material (white arrow) in the peripheral dense material. The images of the first row relate to a control animal, those of the second row to a treated calf.

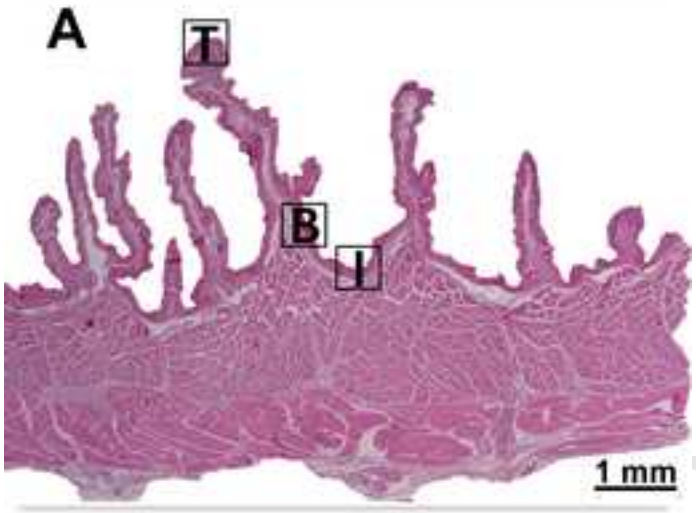

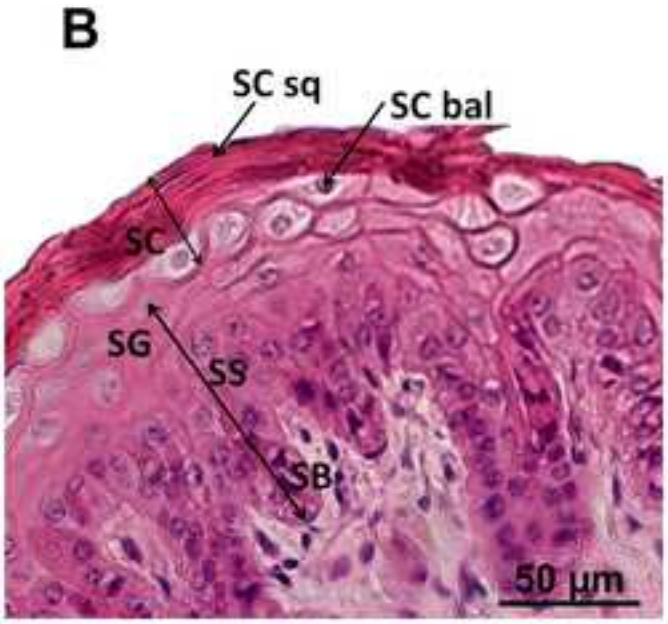

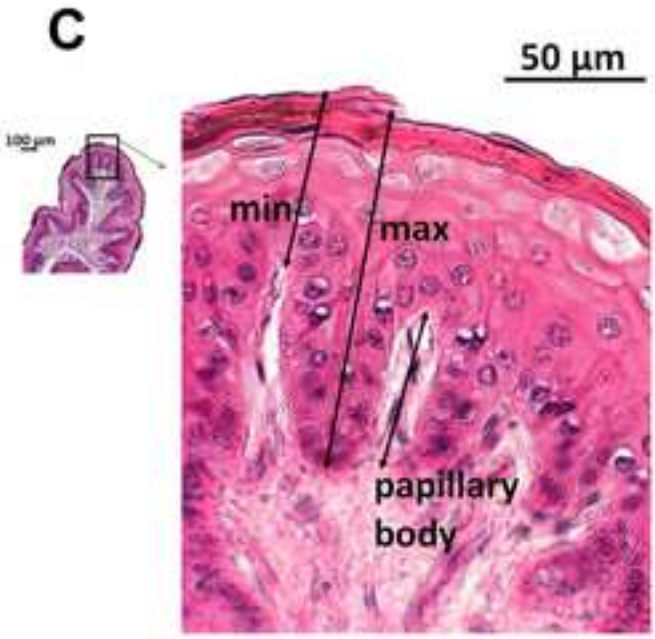

Figure 3

Figure 4

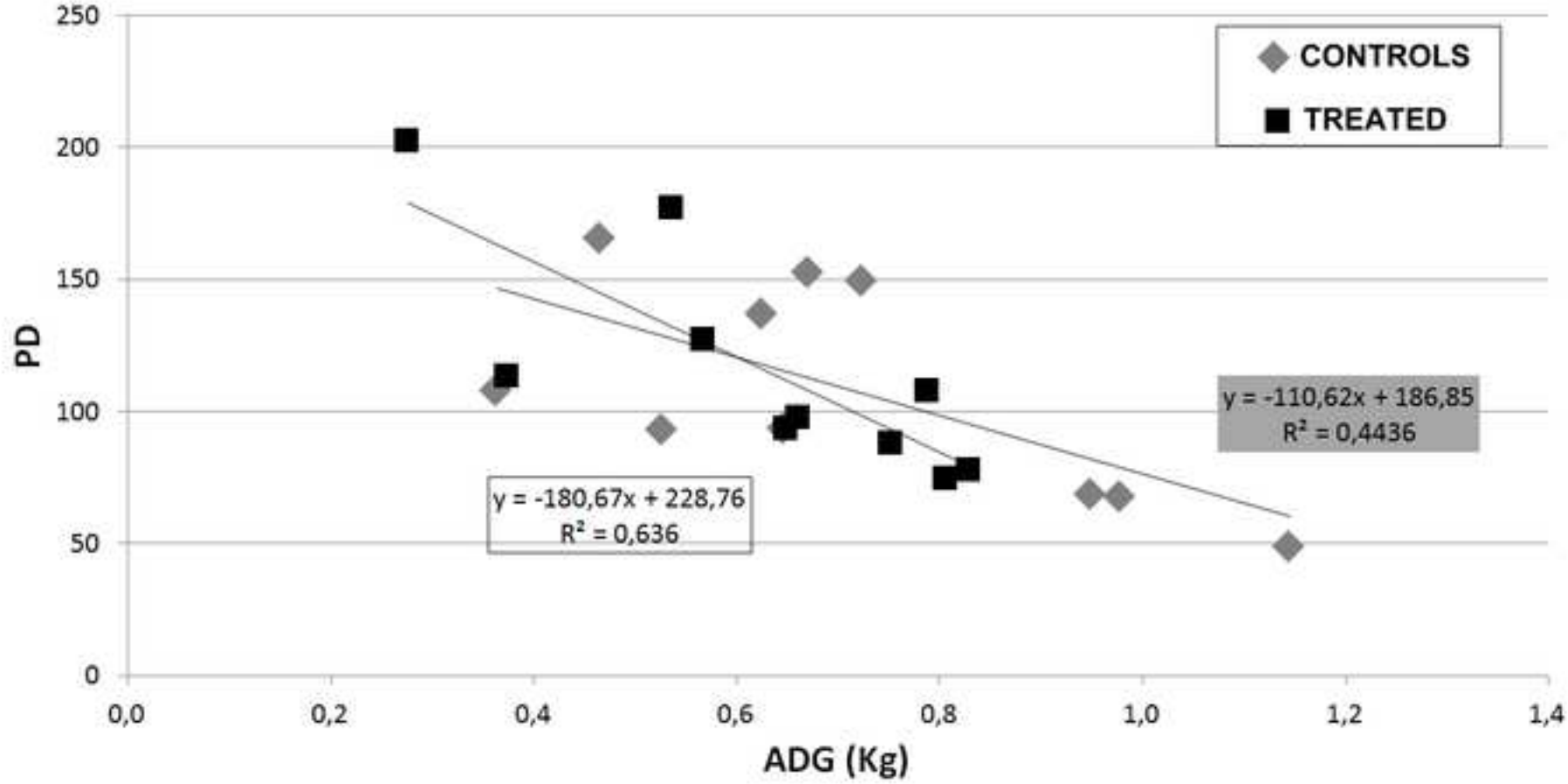
250
200
150
100
50
0
PD
0,0
0,2
0,4
0,6
0,8
1,0
1,2
1,4
ADG (Kg)
CONTROLS
TREATED
y = -110,62x + 186,85
R² = 0,4436
y = -180,67x + 228,76
R² = 0,636

Figure 5

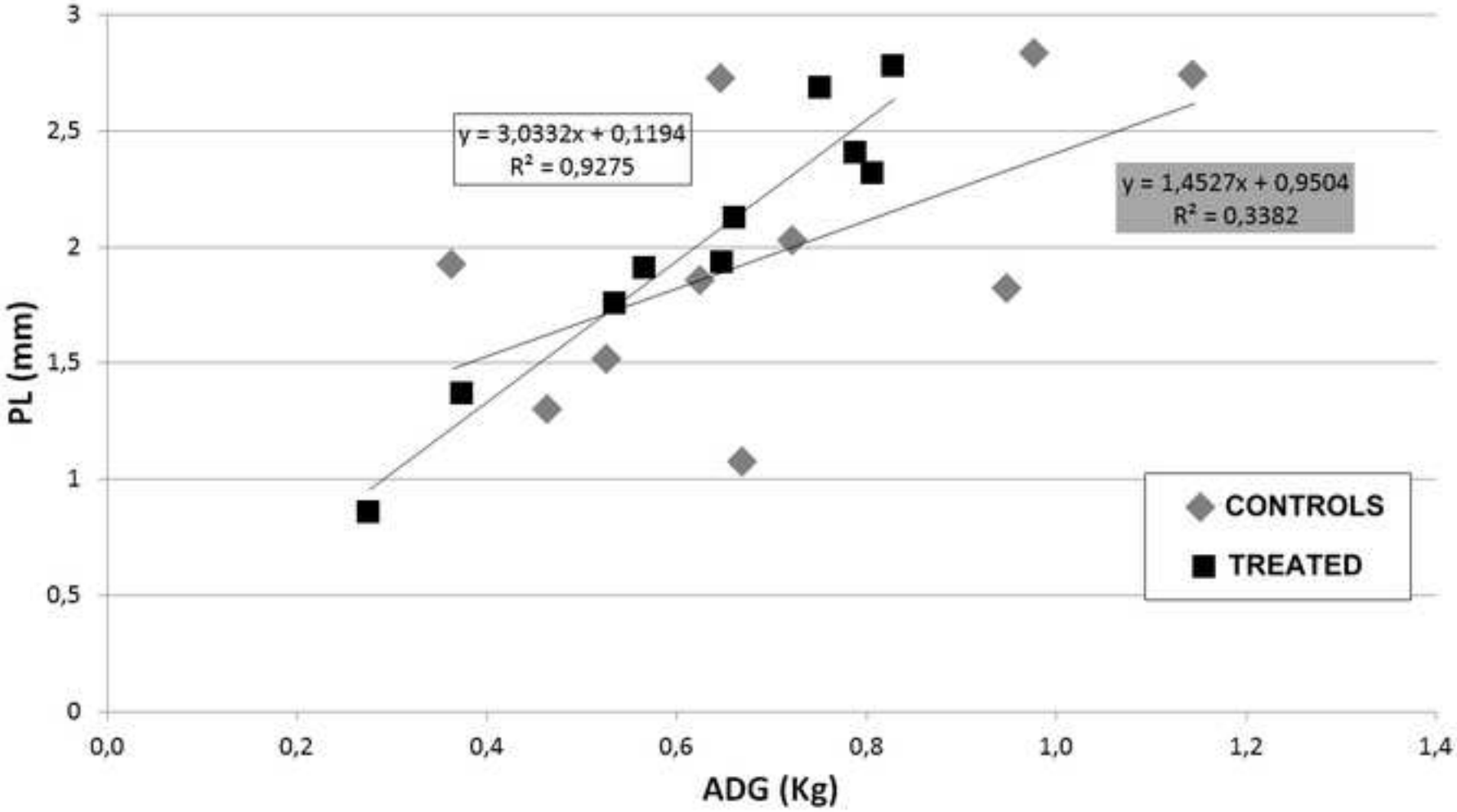
y = 3,0332x + 0,1194
R² = 0,9275
y = 1,4527x + 0,9504
R² = 0,3382
CONTROLS
TREATED
PL (mm)
ADG (Kg)
0
0,5
1
1,5
2
2,5
3
0,0
0,2
0,4
0,6
0,8
1,0
1,2
1,4

Figure 6

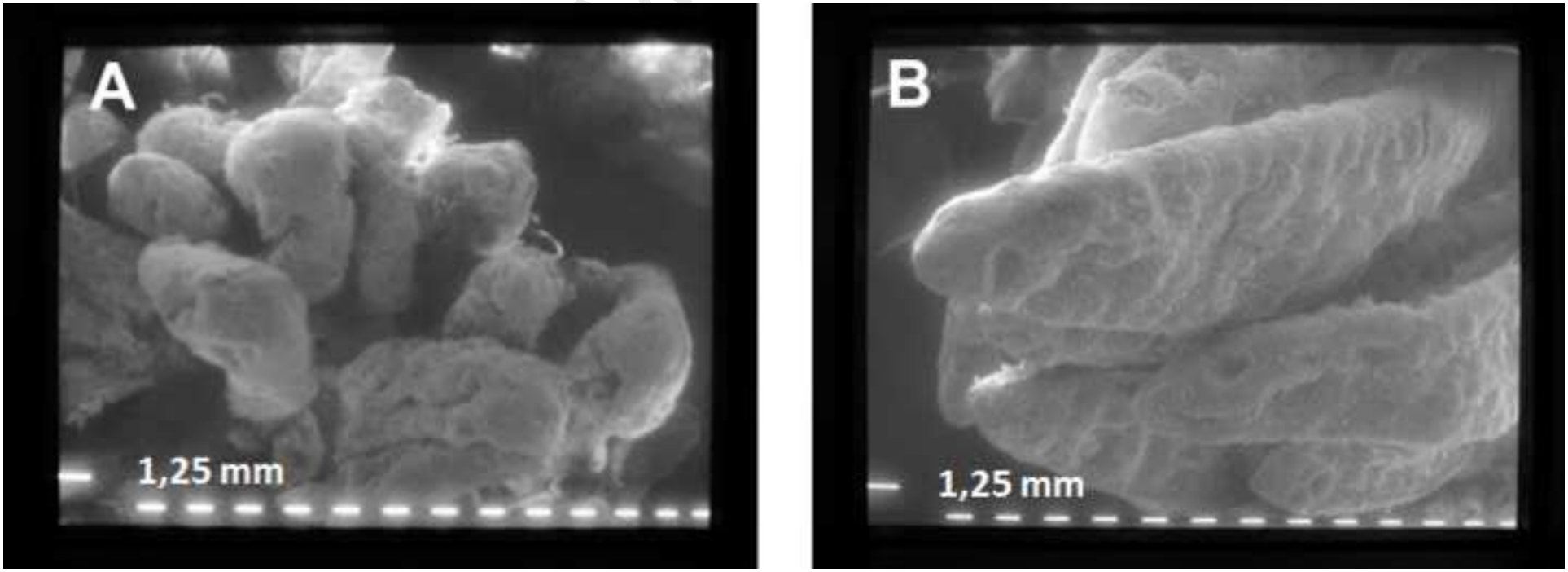

Figure 7

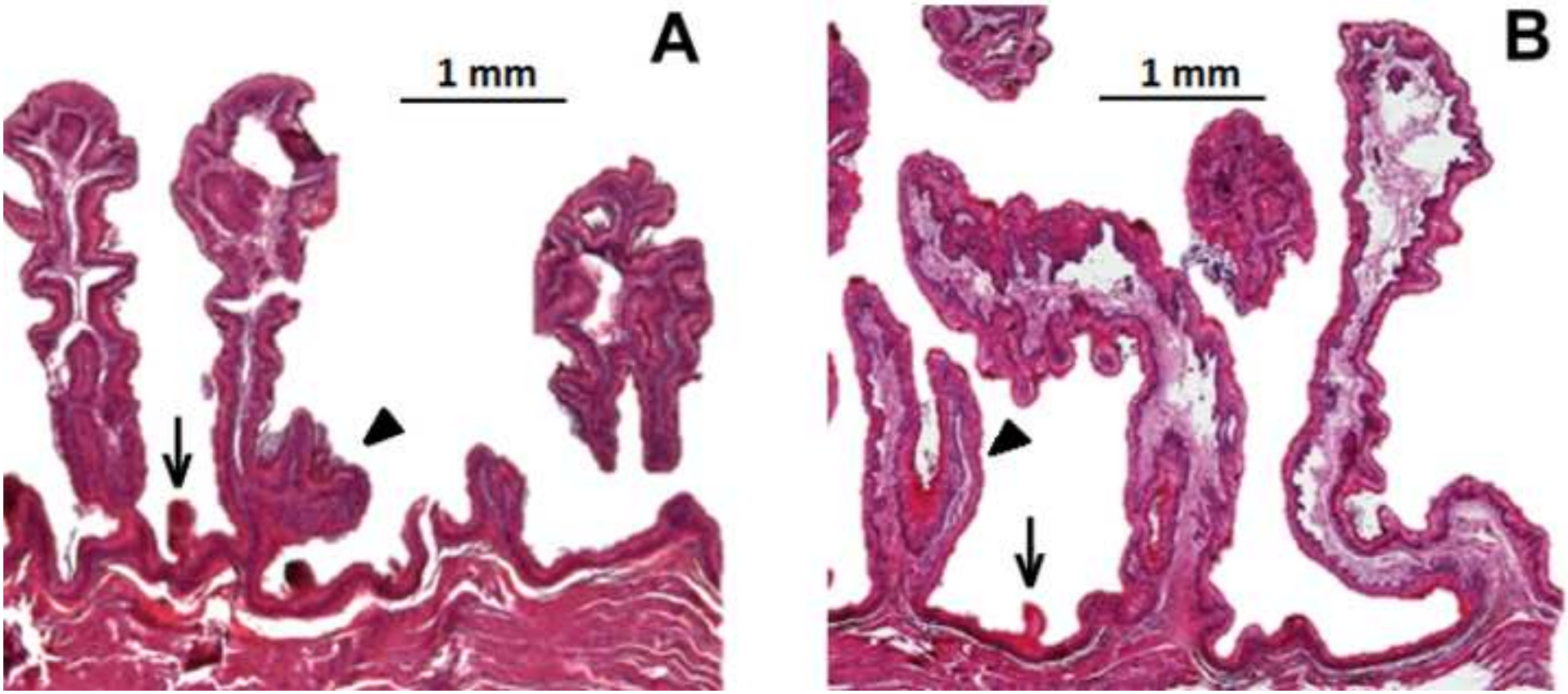

Figure 8

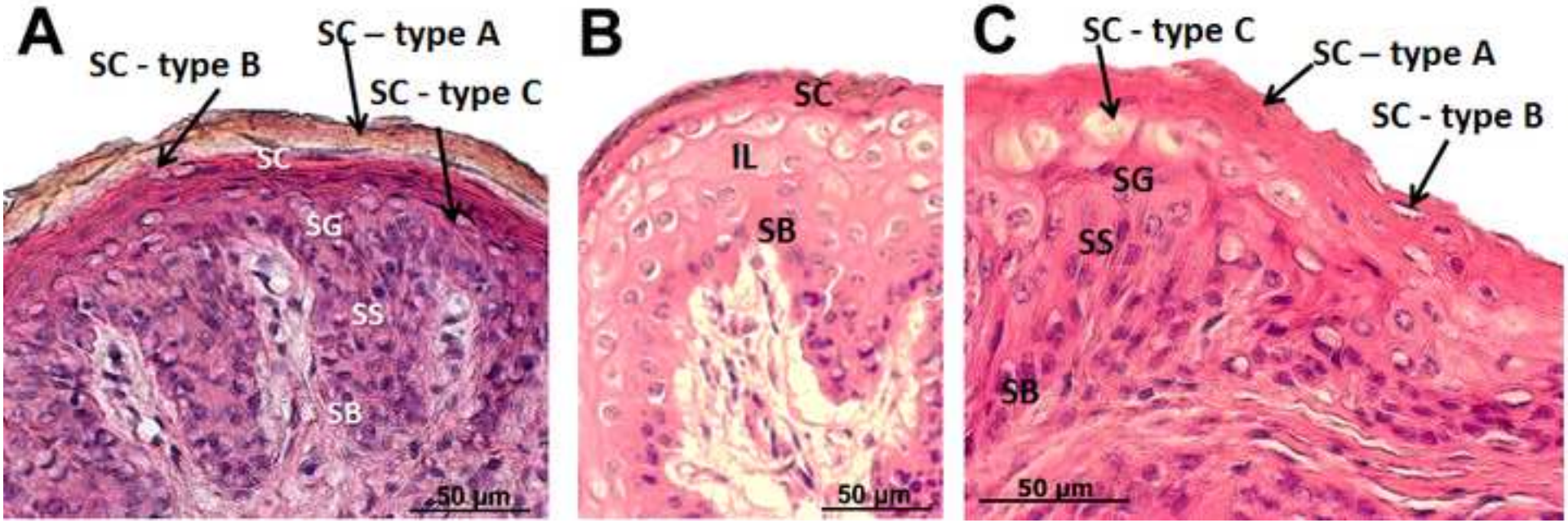

Figure 9

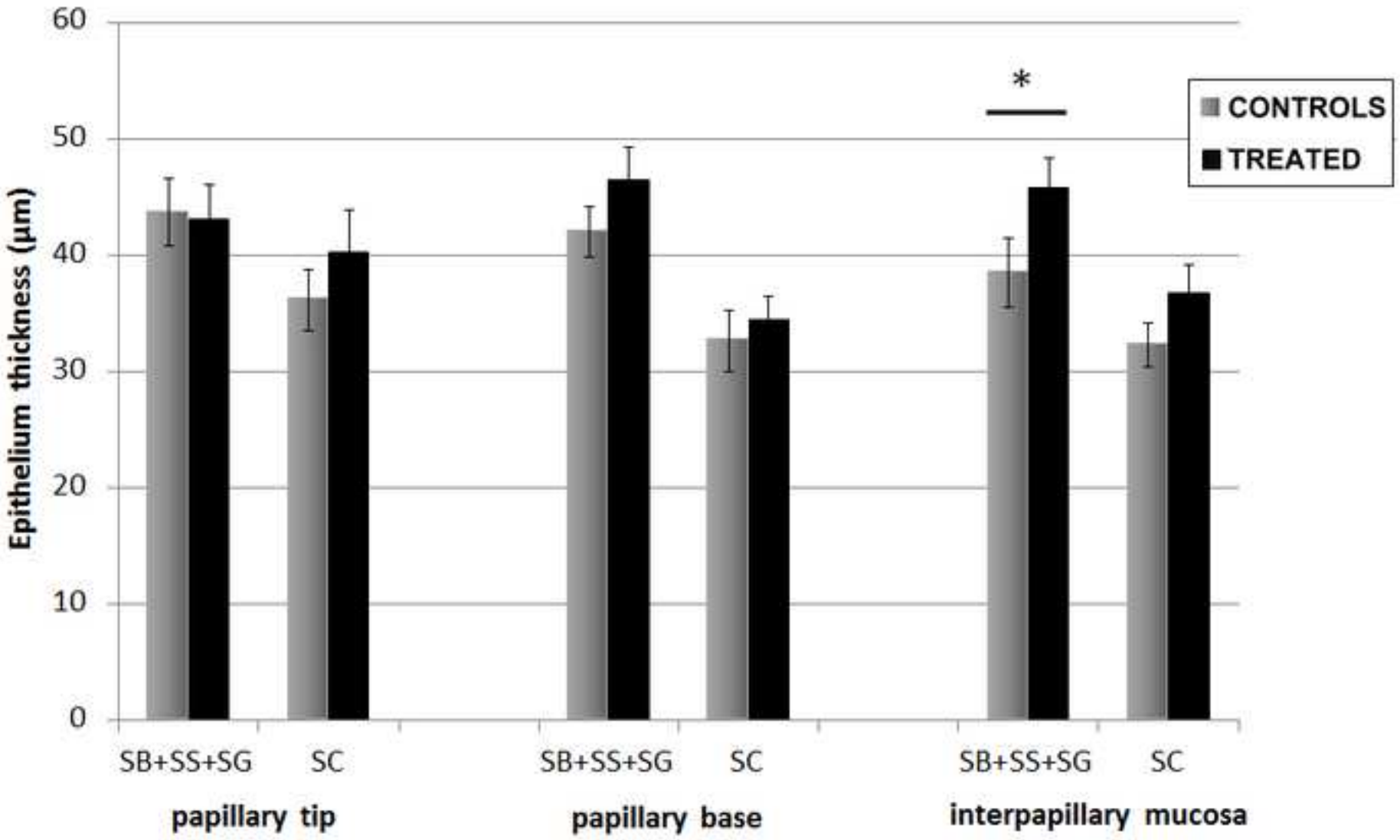
60
50
40
30
20
10
0
Epithelium thickness (µm)
*
CONTROLS
TREATED
SB+SS+SG
SC
SB+SS+SG
SC
SB+SS+SG
SC
papillary tip
papillary base
interpapillary mucosa

Figure 10

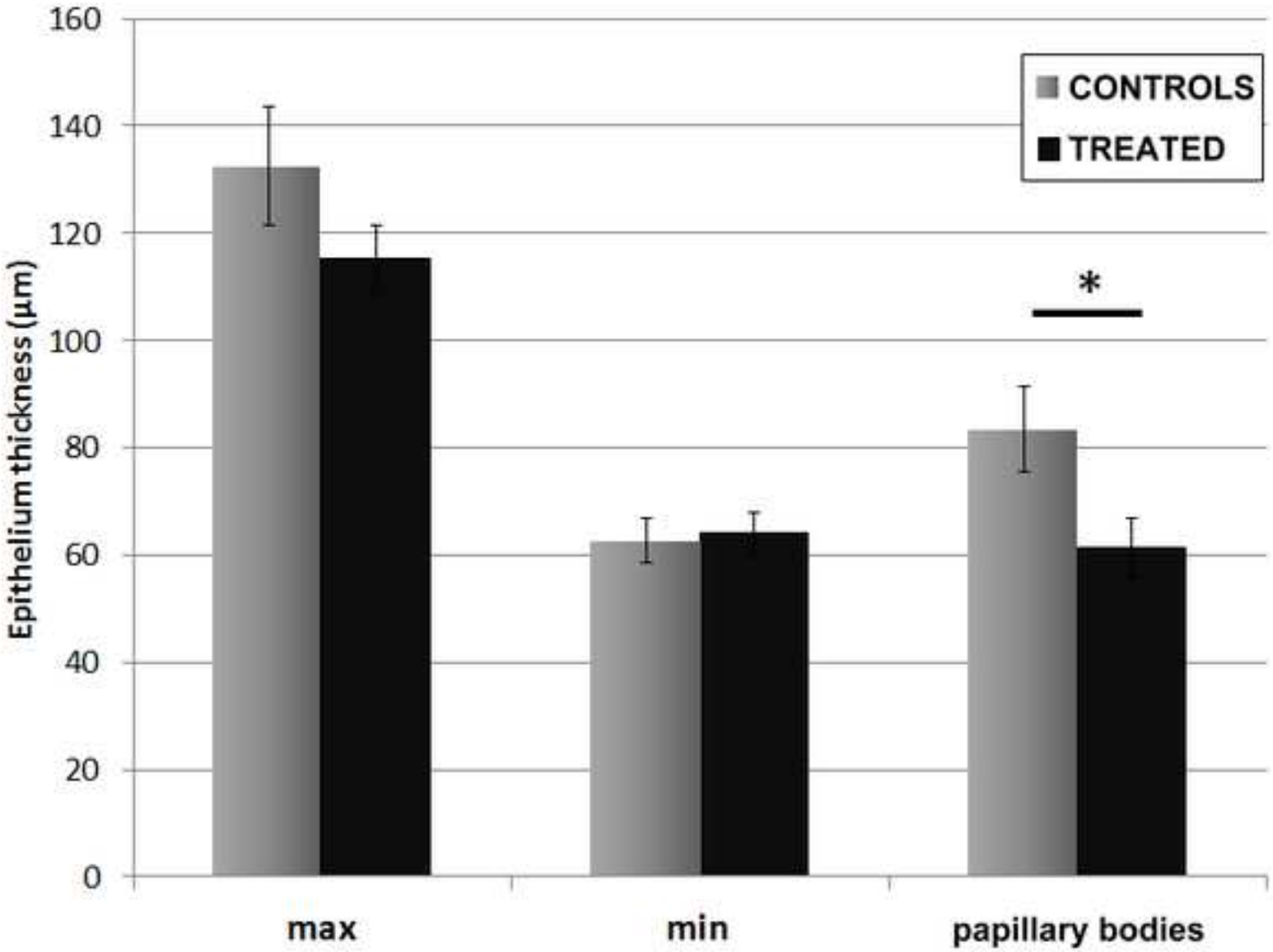
160
140
120
100
80
60
40
20
0
Epithelium thickness (µm)
CONTROLS
TREATED
*
max
min
papillary bodies

Figure 11

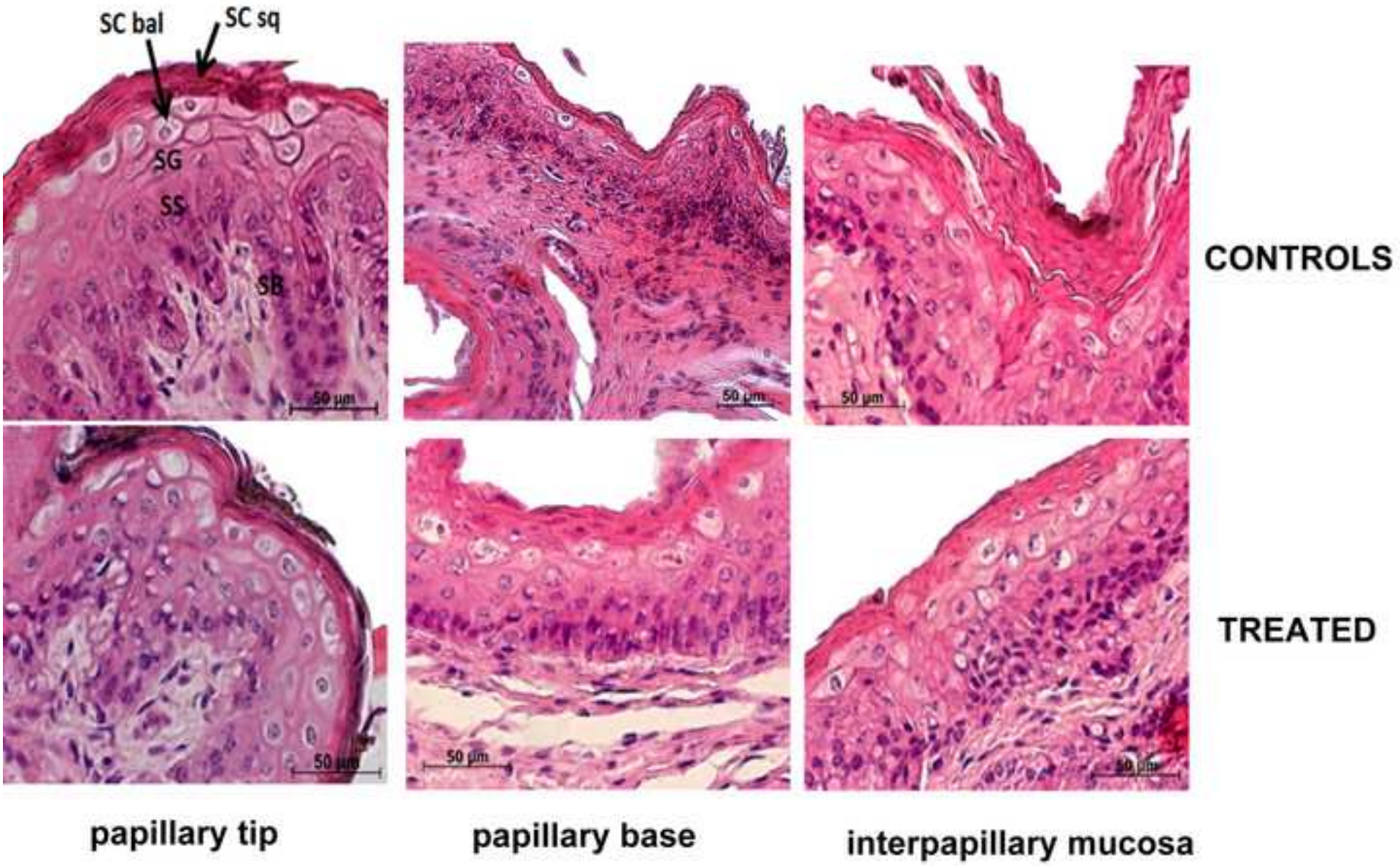
SC bal
SC sq
SG
SS
SB
50 µm
CONTROLS
TREATED
papillary tip
papillary base
interpapillary mucosa

Figure 12

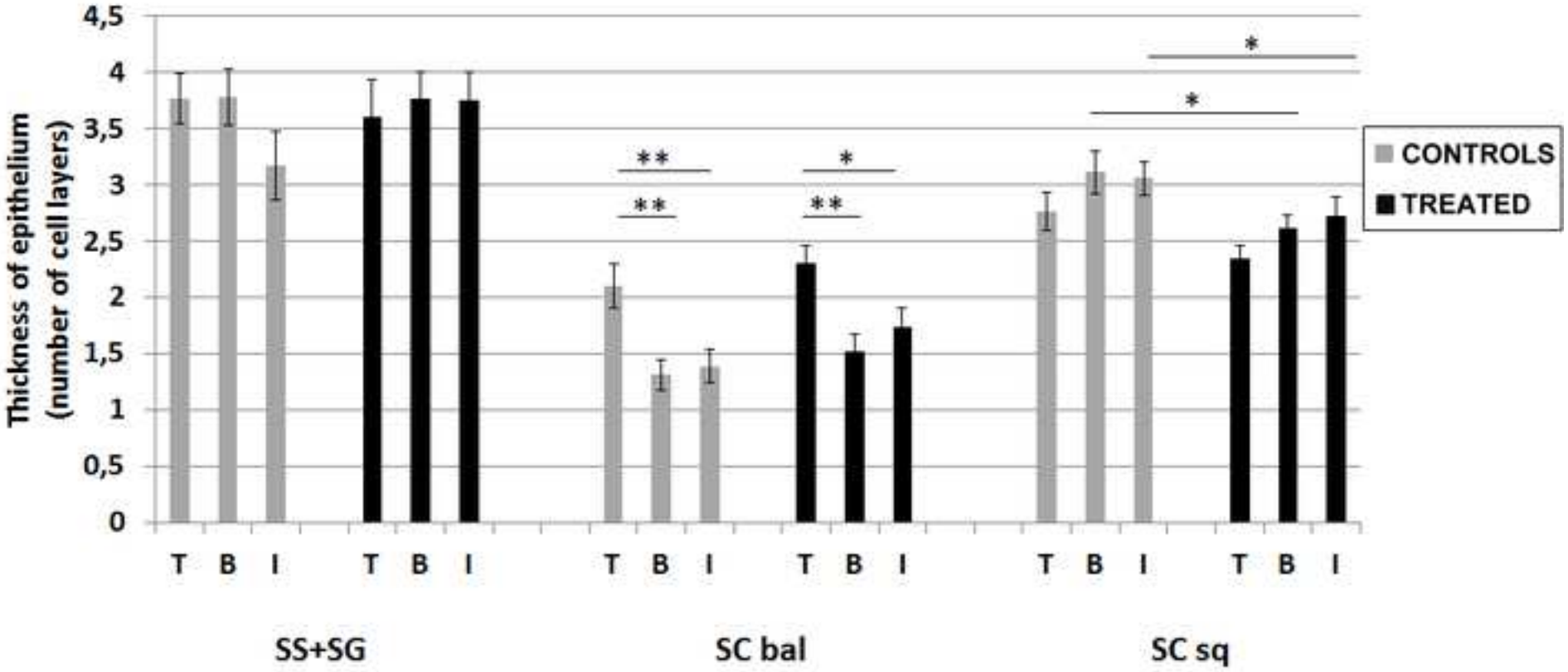
Thickness of epithelium (number of cell layers)
4,5
4
3,5
3
2,5
2
1,5
1
0,5
0
CONTROLS
TREATED
**
**
*
**
*
*
T B I T B I T B I T B I T B I T B I
SS+SG
SC bal
SC sq

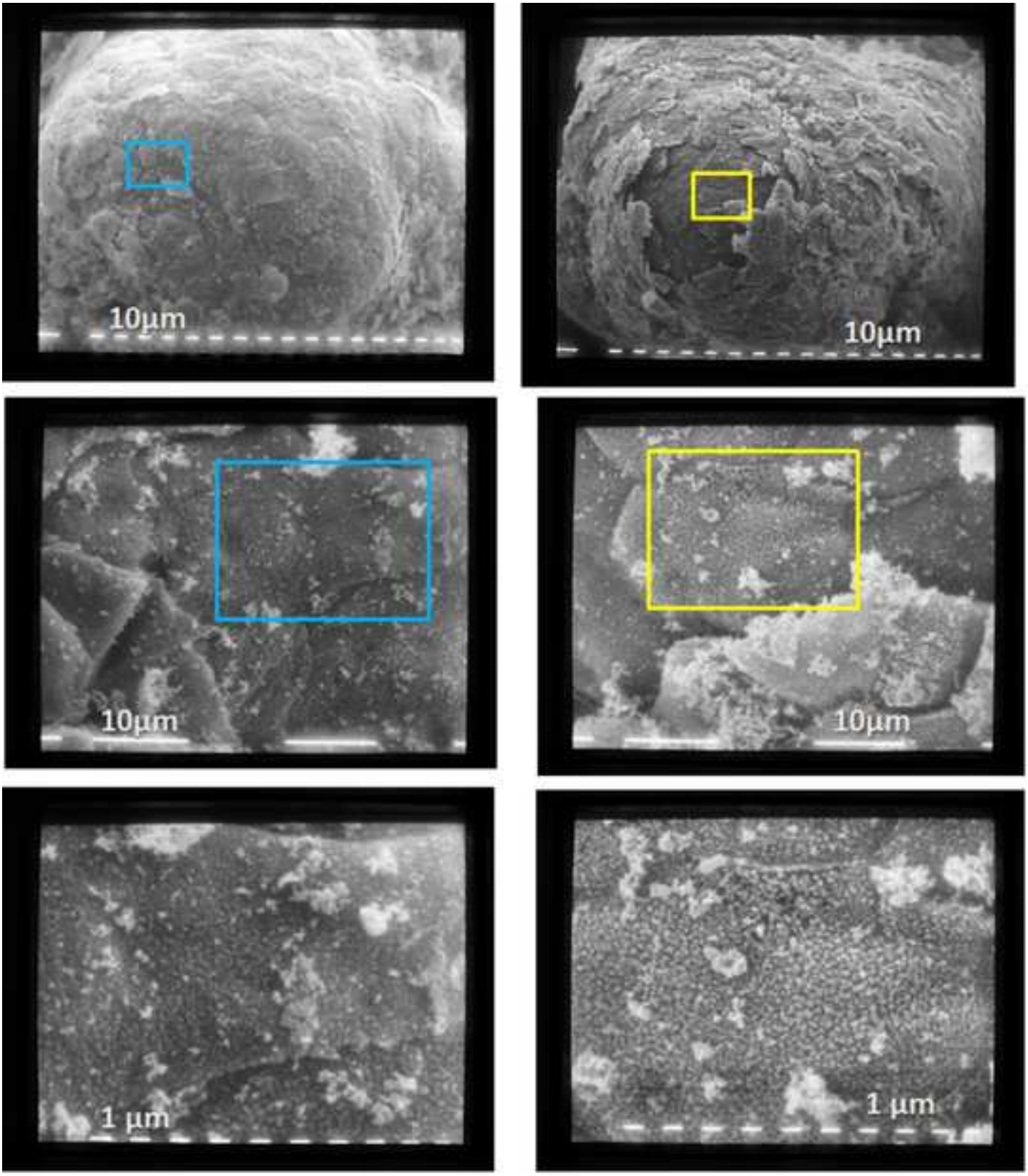

Figure 14

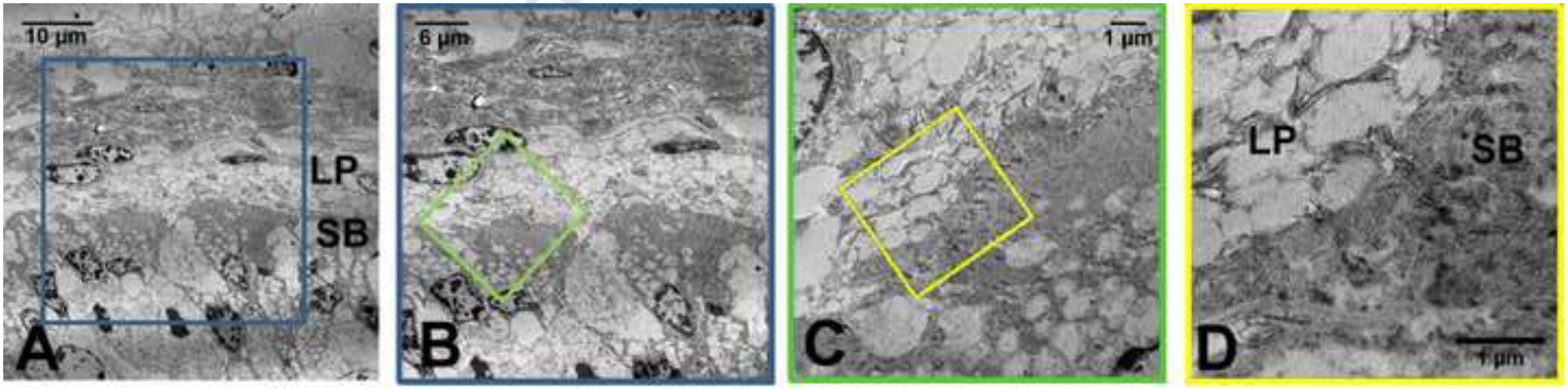

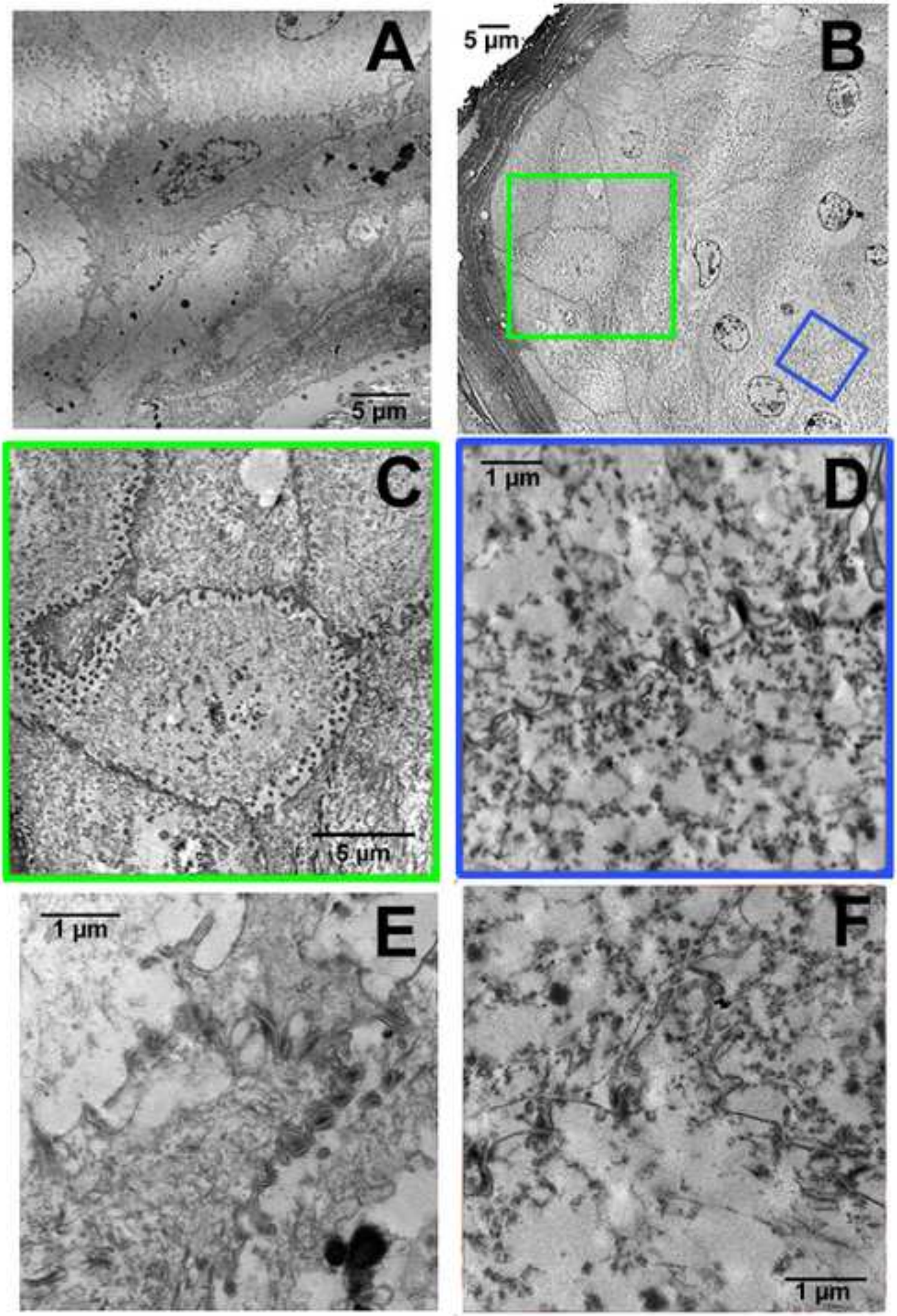

Figure 16